

Imaging Central Nicotinic Acetylcholine Receptors in Baboons with [¹⁸F]Fluoro-A-85380

Héric Valette, Michel Bottlaender, Frédéric Dollé, Ilonka Guenther, Chantal Fuseau, Christine Coulon, Michele Ottaviani and Christian Crouzel

Service Hospitalier Frédéric Joliot, Département de Recherche Médicale, Commissariat à l'Energie Atomique, Orsay, France

Central nicotinic acetylcholine receptors (nAChRs) have been implicated in learning-memory processes. Postmortem brain tissue of patients who suffered senile dementia or Parkinson's disease shows low density of nAChRs. In this study, we used PET to evaluate the distribution and kinetics of the fluoro derivative of the high-affinity and $\alpha 4\beta 2$ -subtype-selective, nicotinic ligand 3-[2(S)-2-azetidylmethoxy]pyridine (A-85380) in baboons. **Methods:** After intravenous injection of 37 MBq (1 mCi, 1–1.5 nmol) [¹⁸F]fluoro-A-85380 into isoflurane-anesthetized baboons, dynamic PET data were acquired for 180 min. Time-activity curves were generated from regions of interest. Displacement experiments (80 min after injection of the radiotracer) were performed using cytisine (1 mg/kg subcutaneously) and unlabeled fluoro-A-85380 (0.1 and 0.3 mg/kg intravenously). Toxicological studies were performed in mice. **Results:** Brain radioactivity reached a plateau within 40–50 min of injection of the tracer. In the thalamic area, radioactivity remained constant for 180 min, while clearance from the cerebellum was slow ($t_{1/2} = 145$ – 190 min). Cytisine and unlabeled fluoro-A-85380 reduced brain radioactivity at 180 min by 50%–60%, 30%–35% and 20%–35% of control values in the thalamus, cerebellum and frontal cortex, respectively. A slight, transient increase (20 mm Hg) in blood pressure was observed with the highest displacing dose of unlabeled fluoro-A-85380. Lethal dose in mice was found to be 2.2 mg/kg intravenously. **Conclusion:** These results demonstrate the feasibility and the safety of imaging nAChRs in vivo using labeled or unlabeled fluoro-A-85380.

Key Words: brain; nicotinic receptors; nonhuman primates; PET; 3-[2(S)-2-azetidylmethoxy]pyridine; [¹⁸F]fluorine

J Nucl Med 1999; 40:1374–1380

Nicotinic acetylcholine receptors (nAChRs) are widely distributed throughout the central and the peripheral nervous system, where they modulate several central nervous system functions including neurotransmitter release, cognitive function, anxiety, analgesia and control of cerebral blood flow. In the brain, a major subtype is composed of the $\alpha 4\beta 2$ subunit combination. Density of this subtype has been shown to be decreased in patients with neurodegenerative disease, such as Alzheimer's disease and Parkinson's disease (1), schizo-

phrenia and epilepsy (2). To study in vivo with PET the evolution of Alzheimer's and Parkinson's disease and the changes in the neuronal biochemistry induced by therapeutic agents, several nicotinic PET ligands have been developed. [¹¹C]nicotine was the first (3,4), but its use is hampered by problems such as nonspecific binding and blood flow dependency (5,6). Compounds chemically related to nicotine (such as [¹¹C] Abbott Laboratories (ABT)-418 [7]) or to cytisine (such as [¹¹C]methylcytisine [7]) were shown to be unsuitable for PET studies of nAChRs. ABT-418 interacted with the central nAChRs for only a short period, whereas methylcytisine did not cross the blood-brain barrier. 3-[(1-[¹¹C]methyl-2(S)-pyrrolidinyl)methoxy]pyridine ([¹¹C]A-84543) (8) seems to be more promising, but only data in mice are available. The most potent ligand has been epibatidine, which has a 40- to 50-pmol/L affinity for central nAChRs (9). It has been successfully labeled with ¹⁸F (10,11) and ⁷⁶Br (12). The addition of a halogen atom to the parent compound did not change the affinity for nAChRs (10,12). Brain kinetics were studied in rodents and baboons. The higher uptake of the ligand was observed in the thalamus, with a thalamus-to-cerebellum radioactivity ratio of approximately 4–7 for the fluorinated and brominated ligands, respectively, 2–3 h after injection (10,12). But the use of epibatidine and [¹⁸F]fluoro-epibatidine creates theoretical (two nicotinic binding sites with different affinity) as well as practical (toxicity) problems (13–16).

A series of nAChR ligands with high affinity has been reported (17). Among them, 3-[2(S)-2-azetidylmethoxy]pyridine (A-85380) showed affinity for nAChRs similar to that of epibatidine. Both compounds competitively displace [³H]cytisine in a concentration-dependent manner with K_i values of 43 and 52 pmol/L for epibatidine and A-85380, respectively (Table 1) (18). [³H]A-85380 binds with high affinity to nAChRs ($K_d = 50$ pmol/L), and specific binding represented 80%–90% of total binding. In vitro kinetic analysis of [³H]A-85380 binding at 37°C revealed association and dissociation half-times favorable for in vivo studies (2.5 and 15.1 min, respectively) (19). A-85380 has an efficacy similar to epibatidine for stimulating ⁸⁶Rb⁺ flux in human $\alpha 4\beta 2$ K177 cells (17). The action of A-85380 at $\alpha 4\beta 2$ was 100-fold lower than that of epibatidine. Furthermore,

Received Sep. 24, 1998; revision accepted Jan. 4, 1999.

For correspondence or reprints contact: Héric Valette, MD, Service Hospitalier Frédéric Joliot, DRM-CEA, 4 Place du Général Leclerc, F-91406 Orsay, France.

TABLE 1
Binding Characteristics of Epibatidine
and [¹⁸F]fluoro-A-85380 at Different Neuronal Acetylcholine
Receptors (nAChRs)

nAChR	A-85380	Epibatidine
K _i α4β2	52 pmol/L	43 pmol/L
K _i α7	148 nmol/L	16 nmol/L
K _i α3βx	0.7 μmol/L	0.007 μmol/L
K _i α1β1δγ	310 nmol/L	2 nmol/L
K _d	50 pmol/L	50 pmol/L

Data from reference 18.

2-fluoro-A-85380 is less toxic than fluoro-epibatidine (lethal dose [LD₅₀] = 7 μmol/kg intravenously in mice and LD₃₀ = 0.5 nmol/kg intravenously in rats [16,20]). [¹⁸F]fluoro-A-85380 has been shown to bind with high affinity to nAChRs in vitro (competitive displacement of [³H]epibatidine in a concentration-dependent manner with a K_i value = 80 pmol/L; RF Dannals, personal communication, April 1998). Furthermore, studies in mice showed high thalamic uptake with a thalamus-to-cerebellum ratio of 20, 180 min after injection of the tracer (20). Such pharmacological properties led us to label A-85380 with ¹⁸F, as done recently by another PET center (21), and to study in vivo the characteristics of the tracer in the mouse and baboon brains.

MATERIALS AND METHODS

Radiosynthesis of [¹⁸F]fluoro-A-85380

[¹⁸F]fluoro-A-85380 has been radiolabeled with no-carrier-added ¹⁸F by nucleophilic aromatic nitro-to-fluoro substitution using [¹⁸F]KF-K₂₂₂ in dimethyl sulfoxide by conventional heating at 150°C for 20 min or by microwave activation at 100 W for 1 min (22). In less than 2 h, 4.1–5.2 GBq (110–140 mCi) [¹⁸F]fluoro-A-85380 could be obtained with specific radioactivities of 111–185 GBq/μmol (3–5 Ci/μmol) calculated for end of bombardment (EOB). Yields (with respect to ¹⁸F ion): decay corrected 49%–64%. Total synthesis time from EOB: 105–110 min. The high-performance liquid chromatography (HPLC)-purified product was found by HPLC analysis to be >98% chemically and radiochemically pure. It was also shown to be radiochemically stable for at least 180 min in physiological saline. Labeling precursor (2-nitro-3-[2(S)-(N-(tert-butoxycarbonyl)-2-azetidylmethoxy)pyridine] and authentic, unlabeled fluoro-A-85380 were prepared as follows. Briefly, Mitsunobu coupling of (S)-N-(tert-butoxycarbonyl)-2-azetidinemethanol and 3-hydroxy-2-nitropyridine or 2-fluoro-3-hydroxypyridine, using diethylazodicarboxylate and triphenylphosphine in tetrahydrofuran at room temperature, gave 2-nitro-3-[2(S)-(N-(tert-butoxycarbonyl)-2-azetidylmethoxy)pyridine] (the labeling precursor) and 2-fluoro-3-[2(S)-(N-(tert-butoxycarbonyl)-2-azetidylmethoxy)pyridine] in 40% and 42% yield, respectively. Trifluoroacetic acid removal of the tert-butoxycarbonyl function gave fluoro-A-85380 in 96% yield.

Animal Studies

Animal use procedures were in accordance with the recommendations of the European Economic Community (86/609/CEE) and

the French National Committee (decret 87/848) for the care and use of laboratory animals.

Studies in Mice. Male Swiss mice weighing 20 g were used in experiments. For kinetics studies, each animal received 0.37 MBq (10 μCi) [¹⁸F]fluoro-A-85380 dissolved in 0.1 mL saline by injection in a tail vein. At designated times (n = 5 mice at 15, 30, 90 and 180 min) after injection of the radiotracer, animals were killed by decapitation, the brains were quickly removed, dissected, weighed and assayed for regional radioactivity. Pretreatment with cytosine (5 mg/kg subcutaneous) or with unlabeled fluoro-A-85380 (0.5 mg/kg intravenous) administered 30 min before injection of the radiotracer was performed. Animals were killed 120 min after injection of the tracer.

A coarse assessment of the acute intravenous toxicity of fluoro-A-85380 was performed in mice. A first dose of 0.275 mg/kg was injected through a tail vein in 10 animals. The injected dose was increased by a factor of two for the next group of 10 animals and so on until the death of all animals receiving the last dose.

PET Studies in Baboons. PET studies of the brain distribution of [¹⁸F]fluoro-A-85380 were performed in adult (mean weight 10 kg) *Papio papio* baboons. Two hours before the PET acquisition the animals received ketamine (10 mg/kg intramuscularly). After being intubated, animals were artificially ventilated and anesthetized with 66% N₂O/1% isoflurane (Ohmeda ventilator OAV 7710; Ohmeda, Madison, WI). PET experiments were performed with an HR+Exact positron tomograph (CTI PET Systems, Knoxville, TN). This scanner allowed simultaneous acquisition of 63 slices every 2.2 mm with spatial and axial resolutions of 4.5 mm. Transmission scans were acquired for 15 min using three retractable ⁶⁸Ge rod sources. The baboon's head was positioned in the tomograph using a custom-designed stereotactic headholder. All the cerebral regions studied (cortex, diencephalon, cerebellum) were contained in axial cross sections parallel to the orbitomeatal anatomic line of reference (23). Baboons (n = 3) were injected intravenous with 37 MBq (1 mCi, 1–1.5 nmol) [¹⁸F]fluoro-A-85380 and imaged for 180 min. The scanning protocol consisted of 33 images (6 × 1 min, 7 × 2 min, 8 × 5 min, 12 × 10 min) for a total duration of 3 h. During PET acquisition, arterial blood samples were withdrawn from the femoral artery at designated times. We examined whether the [¹⁸F]fluoro-A-85380 cerebral uptake could be displaced by injecting cytosine (1 mg/kg subcutaneously, n = 1) or unlabeled fluoro-A-85380 (0.1 or 0.3 mg/kg intravenously, n = 1 for each dose) 80 min after the radiotracer injection. PET imaging was continued for 100 min with the scanning protocol mentioned above. Heart rate and blood pressure (femoral artery) were continuously monitored during the displacement experiments using unlabeled fluoro-A-85380. A presaturation experiment (n = 1) was performed using a dose of 0.2 mg/kg unlabeled fluoro-A-85380 injected as a slow bolus (10 min) 1 h before injection of the radiotracer. This PET experiment lasted 180 min. For PET data analysis, regions of interests were delineated on images on which anatomic structures (frontal cortex, thalamus, cerebellum) could be clearly identified. The concentration of radioactivity in each region of interest was determined during each sequential scan and expressed as percentage of the injected dose per milliliter (%ID/mL) of tissue. Percentage changes in thalamic and cerebellar radioactivities were calculated at the end of the PET experiment (180 min) by dividing the difference in radioactivity (control experiment – challenge experiment) by the value of the radioactivity in the control experiment at 180 min.

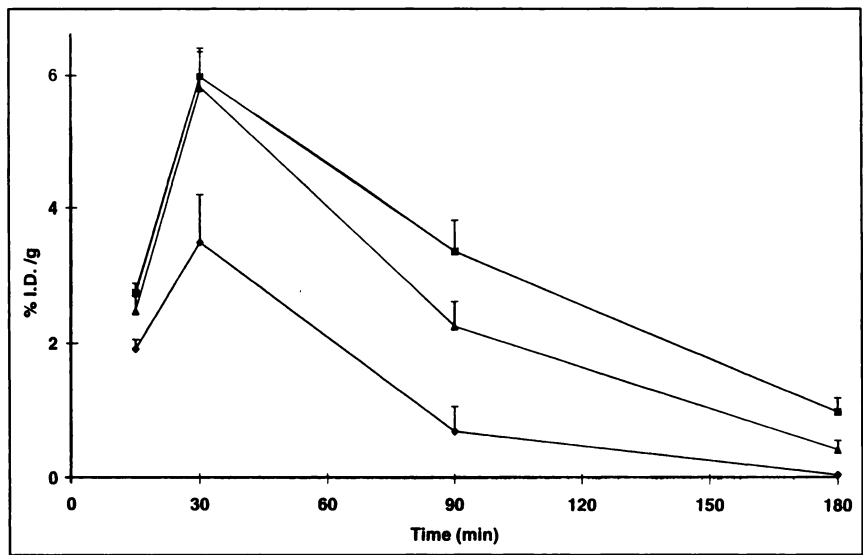


FIGURE 1. Kinetics of radiotracer in mice cerebral structures: thalamus, frontal cortex and cerebellum. Values are mean \pm SDs (n = 5 per point). ■ = thalamus; ▲ = frontal cortex; ◆ = cerebellum.

Determination of Metabolites in Baboons

For analysis of metabolites, arterial blood samples (3 mL) were collected at 1, 2, 5, 11, 19, 27.5, 42.5 and 65 min after injection of the tracer and immediately centrifuged (5 min, 2000g, at 4°C) to obtain cell-free plasma. For deproteinization, 0.5 mL plasma was mixed with 0.7 mL acetonitrile containing fluoro-A-85350 (0.05 mg/mL) as reference compound. After centrifugation at 2000g for 5 min the supernatant (approximately 1.1 mL) was transferred into 1.5-mL microtubes. Acetonitrile was evaporated under reduced pressure using a vacuum centrifuge (Speed vac SVC 1004-220; Bioblock, Illkirch, France, 20-30 min, vacuum 0.01 bar). The remaining samples of 450-500 μ L were directly used for HPLC analysis. The HPLC system consisted of two LC-10AS pumps (Shimadzu, Kyoto, Japan), a 2.6-mL mixing chamber, a Valco injector (model C6W; Valco, Schenkon, Switzerland) with a 1-mL loop and a reverse-phase Waters μ Bondapak C₁₈ column (300 \times 7.8 mm, 10 μ m; Waters, Milford, MA) connected to an ultraviolet detector (Shimadzu SPD-10A; Shimadzu) operated at 254 nm

followed by a radioisotope detector (model LB 506; Berthold, Wildbad, Germany, 500- μ L cell). A Berthold LB 5035 pump was used to add liquid scintillator to the eluent just before the radioactivity detector. The data acquisition and handling were performed on a personal computer with the software Winflow (version 1.21; JMBS Developpements, Grenoble, France). The column was eluted applying a gradient from 5% acetonitrile in 0.01 mol/L phosphoric acid increasing to 35% in 7.5 min, increasing to 50% acetonitrile in 9.5 min, decreasing to 5% acetonitrile at 9.6 min with a total run length of 12 min. The flow rate of the eluent as well as the flow rate of the liquid scintillator was maintained at 6 mL/min.

RESULTS

Studies in Mice

Thalamic uptake of radioactivity peaked at 30 min (5.97 %ID/g) with a thalamus-to-cerebellum ratio of 1.7. Radioac-

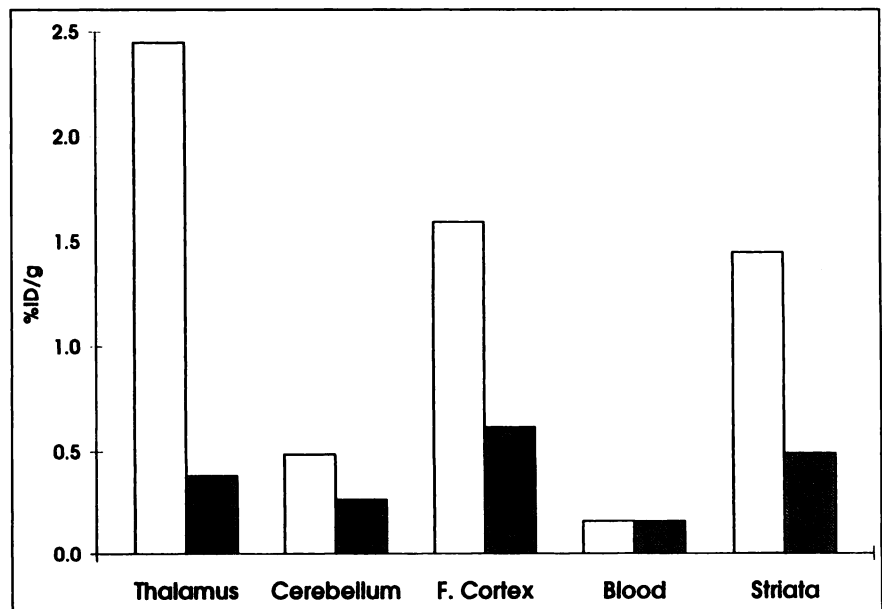


FIGURE 2. Changes in selected cerebral mice structures after pretreatment with cytosine (5 mg/kg subcutaneously).

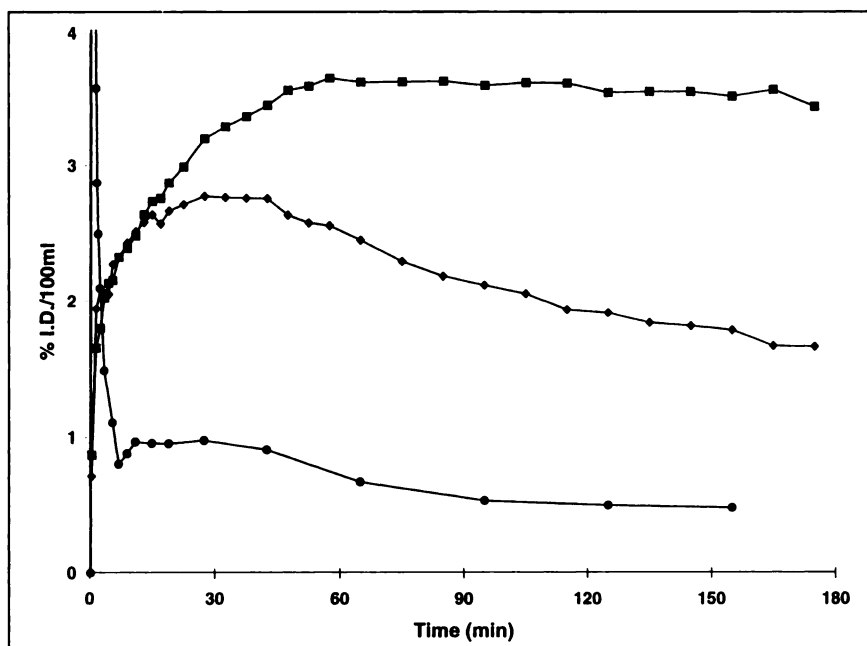


FIGURE 3. Kinetics of radiotracer in baboon cerebral structures: thalamus, cerebellum and plasma. Plasma curve (●) is not corrected for metabolites. ■ = thalamus; ◆ = cerebellum.

tivity in these two structures decreased rapidly (Fig. 1), but the thalamus-to-cerebellum radioactivity ratio increased with time (13.7 at 180 min). Pretreatment with cytosine reduced both thalamic and cerebellar radioactivities by 85% and 46%, respectively (Fig. 2). Pretreatment with unlabeled fluoro-A-85380 reduced both thalamic and cerebellar radioactivities by 76% and 39%, respectively.

LD₁₀₀ was found to be 2.2 mg/kg. At 1.65 mg/kg, all animals had seizures but none died. The maximal dose without any clinical side effect was 1.5 mg/kg.

PET Data in Baboons

Kinetics of the tracer in cerebral structures and in plasma (uncorrected for metabolites) are shown (Fig. 3). Highest radioactivity was found in the thalamus and plateaued from 40 to 180 min with a maximal value of 3.73 ± 0.2 %ID/100 mL tissue (n = 8). Two baboons underwent four PET

examinations each. In the first one, thalamic uptake (80 min postinjection) was 3.81 ± 0.15 %ID/100 mL (range 3.61–3.98 %ID/100 mL). In the second one, the corresponding values (at the same time) were 3.52 ± 0.22 %ID/100 mL (range 3.2–3.72 %ID/100 mL). Peak radioactivity in the cerebellum was 2.67 ± 0.13 %ID/100 mL tissue (n = 8). Clearance from cerebellum was slow ($t_{1/2} = 2.5$ –3 h). The thalamus-to-cerebellum radioactivity ratio increased slightly with time: 1.8 ± 0.07 at 80 min and 2.1 ± 0.06 at 180 min (n = 2). Injection of cytosine (Fig. 4) displaced 52% of thalamic radioactivity, whereas 23% of cerebellar radioactivity was displaced at 180 min postinjection (data obtained in the same baboon in two separate experiments) (Table 2). Injection of unlabeled fluoro-A-85380 (Fig. 5) (0.1 or 0.3 mg/kg intravenously, n = 1 for each dose) displaced thalamic radioactivity by 53% and 63% at 180 min postinjec-

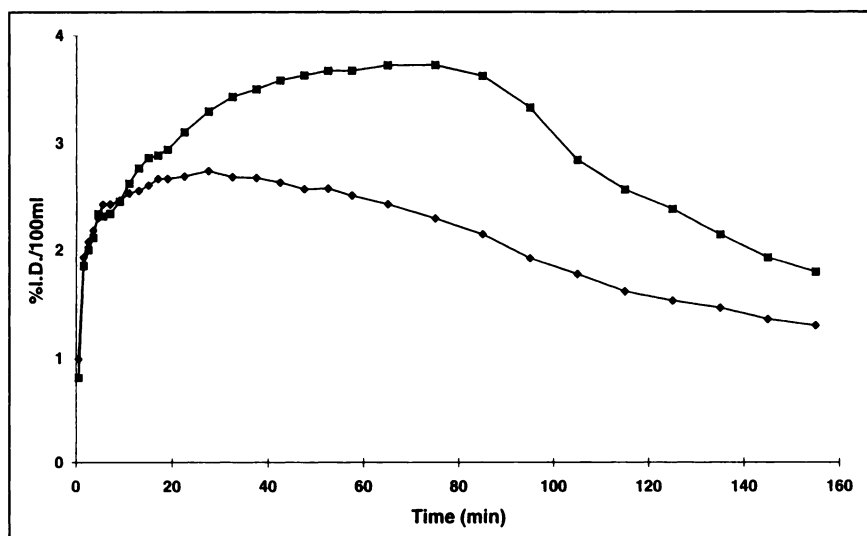


FIGURE 4. Displacement by cytosine (1 mg/kg subcutaneously) injected at 80 min. ■ = thalamus; ◆ = cerebellum.

TABLE 2
Percentage Changes at 180 Min in Selected Baboon Cerebral Structures Induced by Administration of Fluoro-A-85380 and Cytisine During PET Experiments

Structure	Displacement by fluoro-A-85380		Displacement by cytisine 1 mg/kg
	0.1 mg/kg	0.3 mg/kg	
Thalamus	53%	63%	52%
Cerebellum	26%	31%	23%
Frontal cortex	20%	35%	22%

tion, respectively (Table 2). At these doses, cerebellar radioactivity was displaced by 26% and 31%, respectively. No changes in hemodynamic parameters (monitoring of femoral artery pressure) were observed within 1 h of intravenous injection of 0.1 mg/kg unlabeled fluoro-A-85380. After the higher dose (0.3 mg/kg), a transient increase (20 mm Hg) in blood pressure was observed for 10 min and the blood pressure returned to control values in 10 min. Heart rate remained unchanged with both doses. Presaturation with unlabeled fluoro-A-85380 reduced thalamic and cerebellar uptake by 70% and 40%, respectively, 180 min after injection of the radiotracer (Table 2). Thalamic and cerebellar time-activity curves were superimposed. A slight increase in blood pressure (10 mm Hg) was observed at the end of the perfusion of the unlabeled compound. Blood pressure returned to control values 5 min after the end of the perfusion.

The analysis of plasma showed that 85% of the radioactivity was recovered in the supernatant after protein precipitation. Preliminary metabolite analysis revealed a relatively slow metabolism of fluoro-A-85380 (Fig. 6): 80 min after tracer injection, $55.5\% \pm 3.7\%$ of the activity in plasma belonged to unchanged tracer ($n = 3$). A metabolite (retention time [RT] 4.0 min) found in plasma was more hydro-

philic than the parent compound (RT 4.6 min) and accounted for $20.5\% \pm 0.8\%$ of the activity at the same time point, whereas three minor, more lipophilic metabolites (RT 5.0, 6.7 and 7.3 min) accounted for $23.9\% \pm 4.5\%$ (sum of the three metabolites; $n = 1-4$ baboons) of the total activity in plasma.

DISCUSSION

In this study, the kinetics and regional brain distribution of a fluorinated analog of A-85380 were assessed using PET in baboons. This compound is likely to be a nicotinic ligand because, in mice, presaturation with cytisine strongly decrease thalamic uptake. A similar decrease (88%) (20) in the thalamic radioactivity was found in CD-1 mice after the administration of the same amount of cytisine. Although the cerebellum is an nAChR-poor area, specific binding was demonstrated *in vivo* in this structure for nicotine (7). In this study, a reduction (46%) of cerebellar uptake after pretreatment with cytisine was observed; a similar value (40%) was reported in CD-1 mice using the same dose of cytisine (RF Dannals, personal communication, November 1998). This fact differentiates fluoro-A-85380 from fluoro-epibatidine (10). Presaturation experiments by unlabeled fluoro-A-85380 showed a residual binding in the thalamus of 25%. In this cerebral structure, the corresponding value in baboons is 30%. In the cerebellum, uptake of the radiotracer was reduced by only 40%, suggesting a higher nonspecific binding than that observed with fluoro-epibatidine (24). We could use unlabeled fluoro-A-85380 for displacement and presaturation experiments because its acute intravenous toxicity in mice appeared to be clearly lower than that of other nicotinic PET ligands. The first dose we used in baboons was chosen as one tenth of the higher dose, which did not produce a clinical side effect in mice. Using this dose, no clinical or hemodynamic effect was observed in

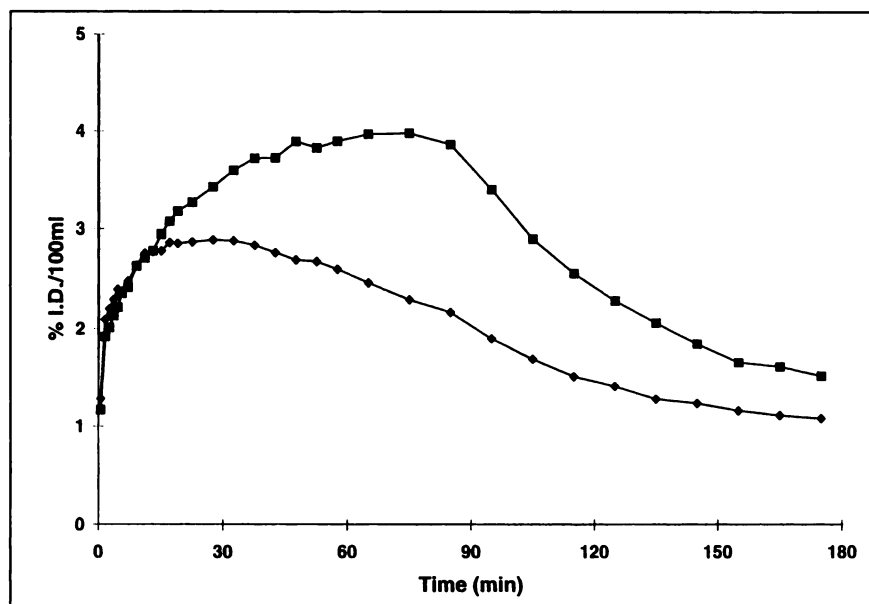


FIGURE 5. Displacement by unlabeled fluoro-A-85380 (0.3 mg/kg intravenously) injected at 80 min. ■ = thalamus; ◆ = cerebellum.

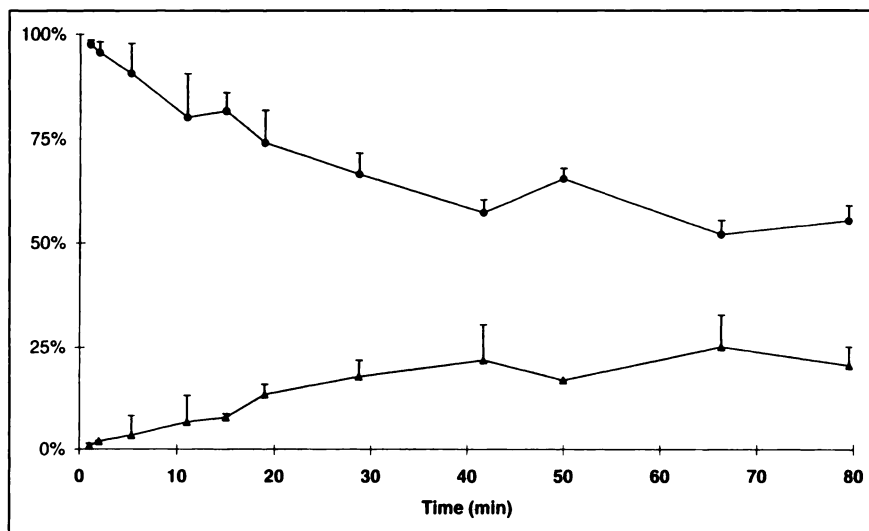


FIGURE 6. Unchanged (●) fluoro-A-85380 and lipophilic metabolites (sum of three lipophilic metabolites, ▲) of fluoro-A-85380 within 80 min of injection of tracer. Data concerning hydrophilic metabolite are not shown because time-activity curve is almost superimposed to one of lipophilic metabolites. Values are mean \pm SD ($n = 1-4$ baboons).

baboons. When the dose was increased three-fold, only a slight transient increase in blood pressure was observed. Therefore, the use of fluoro-A-85380 appears to be relatively safe in anesthetized nonhuman primates. The metabolism of fluoro-A-85380 is rather slow, but the three lipophilic metabolites (chemically unknown) detected in plasma could cross the blood-brain barrier and therefore could contribute to nonspecific binding.

Brain kinetics of [18 F]fluoro-A-85380 are strikingly different in mice and baboons. Although there are species differences in the distribution of central nAChRs in mammalian brain (25,26), the effects of anesthesia cannot be ruled out. Volatile, halogenated anesthetic agents have been shown to stabilize the slow desensitized conformational state of nAChRs, an inactive state characterized by high affinity for agonists (27,28). The $\alpha 4\beta 2$ nAChRs are especially affected by isoflurane, the anesthetic agent used in this study. The changes in nAChR affinity induced by isoflurane can also explain the difference in the shape of thalamic time-activity curves. In nAChR-rich areas in anesthetized baboons, the kinetics of [18 F]fluoro-A-85380 are slow, a possible drawback for clinical use (if the brain kinetics of the tracer are similar in humans). Two injections of the radiotracer are usually performed for quantification of receptors. The second injection is performed when equilibrium is reached. For fluoro-A-85380, this equilibrium is reached in baboons at 100–140 min. Such slow kinetics suppose a PET acquisition lasting at least 200 min, which seems long for patients with senile dementia.

In vitro studies have shown that A-85380 competitively displaced [3 H]cytisine from $\alpha 4\beta 2$ nAChR subtype in a concentration-dependent manner consistent with a single site competitive model with K_i values of 52 pmol/L (18). [18 F]fluoro-A-85380 binding to nAChRs also exhibits pharmacological specificity. After administration of cytisine in vivo, a marked decrease in [18 F]fluoro-A-85380 binding was observed in nAChR-rich regions. This displacement was not observed in the eyes, where the nicotinic-bungarotoxin

receptor subtype is abundant (29). Therefore, fluoro-A-85380 also showed a specific binding for $\alpha 4\beta 2$ nAChRs.

The brain kinetics of [18 F]fluoro-A-85380 in isoflurane-anesthetized *Papio papio* is similar to that observed with [18 F]fluoroepibatidine (24) in *Papio anubis* anesthetized with alfaxalone acetate and alfadolone (steroid derivatives). These neurosteroids did not affect binding properties of [3 H]nicotine in vitro (30). In the study by Villemagne et al. (24), as in this study, a plateau was also observed in the thalamus (1.4 %ID/100 mL tissue) 40 min after injection of the tracer, whereas clearance ($t_{1/2}$) from the cerebellum was more rapid (approximately 3 h). A higher amount of radioactivity (67%) was displaced in the thalamus after injection of cytisine. In contrast, [18 F]fluoroepibatidine injected into isoflurane-anesthetized *Papio anubis* had completely different brain kinetics (11). Radioactivity (0.06 %ID/g) in the thalamus peaked 5–10 min after injection of the radiotracer. Clearance from the thalamus and the cerebellum was faster ($t_{1/2} = 170$ and 25 min, respectively). These discrepancies underline the possible effects of anesthetic agents and the species differences on the kinetics of these ligands.

CONCLUSION

The results obtained in mice and baboons demonstrate the feasibility and relative safety of nAChRs in in vivo imaging using [18 F]fluoro-A-85380. Other studies to characterize this radiotracer are needed.

REFERENCES

1. Rinne JO, Myllykylä R, Lönnberg P, Marjamäki P. A postmortem study of brain nicotinic receptors in Parkinson's and Alzheimer's disease. *Brain Res.* 1991;547:167–170.
2. Gotti C, Fornasari D, Clementi F. Human neuronal nicotinic receptors. *Prog Neurobiol.* 1997;53:199–237.
3. Maziere M, Comar D, Marazano C, Berger G. Nicotine 11 C: synthesis and distribution kinetics in animals. *Eur J Nucl Med.* 1976;1:255–258.
4. Halldin C, Nagren K, Swahn C-G, Langström B, Nybäck H. (S)- and (R)-(11 C)nicotine and the metabolite (R/S)-(11 C) cotinine. Preparation, metabolite

- studies and in vivo distribution in the human brain using PET. *Nucl Med Biol.* 1992;19:871–880.
5. Nybäck H, Halldin C, Ahlin A, Curvall M, Eriksson L. PET studies of the uptake of (S)- and (R)-¹¹C-nicotine in the human brain: difficulties in visualizing specific receptor binding in vivo. *Psychopharmacology.* 1994;115:31–36.
 6. Broussolle EP, Wong DF, Fanelli RJ, London ED. In vivo specific binding of ³H-nicotine in the mouse brain. *Life Sci.* 1989;44:1123–1132.
 7. Valette H, Bottlaender M, Dollé F, Dolci L, Syrota A, Crouzel C. An attempt to visualize baboon brain nicotinic receptors with N-[¹¹C]ABT-418 and N-[¹¹C] methyl-cytisine. *Nucl Med Commun.* 1997;18:164–168.
 8. Kassiou M, Scheffel UA, Ravert HT, et al. Pharmacological evaluation of [¹¹C]A-84543: an enantioselective ligand for in vivo studies of neuronal nicotinic acetylcholine receptors. *Life Sci.* 1998;63:PL13–PL18.
 9. Badio B, Daly JW. Epibatidine: a potent analgesic and nicotinic agonist. *Mol Pharmacol.* 1994;45:563–569.
 10. Horti A, Scheffel U, Stathis M, et al. Fluorine-¹⁸FHP for PET imaging of nicotinic acetylcholine receptors. *J Nucl Med.* 1997;38:1250–1265.
 11. Ding YS, Gatley SJ, Fowler JS, et al. Mapping nicotinic acetylcholine receptors with PET. *Synapse.* 1996;24:403–407.
 12. Bottlaender M, Loc'h C, Kassiou M, et al. In vivo PET study of nicotinic acetylcholine receptors (nAChR) with [⁶Br]bromoepibatidine [abstract]. *Soc Neurosci Ann Meeting.* 1997;23:382.
 13. Fisher M, Huangfu D, Shen TY, Guyenet PG. Epibatidine: an alkaloid from the poison frog *Epipedobates tricolor* is a powerful ganglionic depolarizing agent. *J Pharmacol Exp Ther.* 1994;270:702–707.
 14. Houghtling RA, Dávila-García MI, Hurt SD, Kellarv KJ. [³H]epibatidine binding to nicotinic cholinergic receptors in brain. *Med Chem Res.* 1994;4:538–546.
 15. Lukas RJ. Expression of ganglia-type nicotinic acetylcholine receptors and nicotinic binding sites by cells of the IMR-32 human neuroblastoma clonal line. *J Pharmacol Exp Ther.* 1993;265:294–302.
 16. Molina PE, Ding YS, Carrol I, et al. Fluoro-norchloroepibatidine: preclinical assessment of acute toxicity. *Nucl Med Biol.* 1997;24:743–747.
 17. Abreo MA, Lin NH, Garvey DS, et al. Novel 3-pyridyl ethers with subnanomolar affinity for central neuronal nicotinic acetylcholine receptors. *J Med Chem.* 1996;39:817–825.
 18. Sullivan JP, Donnelly-Roberts DL, Briggs CA, et al. A-85830 [3-(2(S)-azetidylmethoxy)pyridine]: in vitro pharmacological properties of a novel high affinity alpha4 beta2 nicotinic acetylcholine receptor ligand. *Neuropharmacol.* 1996;35:725–734.
 19. Anderson DJ, Campbell JE, Raszkievicz JL, et al. Binding properties of [³H]A-85380: a high-affinity neuronal nicotinic acetylcholine receptor radioligand [abstract]. *Soc Neurosci Ann Meeting.* 1995;21:606.
 20. Horti AG, Koren AO, Scheffer U, et al. 2[¹⁸F]Fluoro-5-(2(S)-azetidylmethoxy)pyridine, a radioligand for in vivo imaging of central nicotinic receptors [abstract]. *Soc Neurosci Ann Meeting.* 1997;23:382.
 21. Horti AG, Koren AO, Ravert HT, et al. Synthesis of a radiotracer for studying nicotinic acetylcholine receptors: 2[¹⁸F]-3-[2(S)-azetidylmethoxy]pyridine (2-[¹⁸F]-A-85380). *J Labelled Compd Radiopharm.* 1998;41:309–318.
 22. Dollé F, Valette H, Bottlaender M, et al. Synthesis of 2-[¹⁸F]fluoro3-[2(S)-azetidylmethoxy]pyridine: a highly potent radioligand for in vivo imaging central nicotinic acetylcholine receptors. *J Labelled Compd Radiopharm.* 1998;41:451–463.
 23. Riche D, Hantraye P, Guibert B, et al. Anatomical atlas of the baboon's brain in the orbito-meatal plane used in experimental positron emission tomography. *Brain Res Bull.* 1988;20:283–287.
 24. Villemagne VL, Horti A, Scheffel U, et al. Imaging nicotinic acetylcholine receptors with fluorine-18-FPH: an epibatidine analog. *J Nucl Med.* 1997;38:1737–1741.
 25. Nordberg A, Alafuzoff I, Winblad B. Nicotinic and muscarinic subtypes in the human brain: changes with aging and dementia. *J Neurosci Res.* 1992;31:103–111.
 26. Cimino M, Marini P, Fornasari D, Cattabeni F, Clementi F. Distribution of nicotinic receptors in cynomolgus monkey brain and ganglia: localization of alpha 3 subunit mRNA, alpha-bungarotoxin and nicotine binding sites. *Neuroscience.* 1992;51:77–86.
 27. Violet JM, Downie DL, Nasika RC, Lieb WR, Franks NP. Differential sensitivities of mammalian neuronal and muscle nicotinic acetylcholine receptors to general anesthetics. *Anesthesiology.* 1997;86:866–874.
 28. Flood P, Ramirez-Latorre J, Role L. $\alpha 4\beta 2$ neuronal nicotinic acetylcholine receptors in the central nervous system are inhibited by isoflurane and propofol, but $\alpha 4$ -type nicotinic acetylcholine receptors are unaffected. *Anesthesiology.* 1997;86:859–865.
 29. McKay J, Lindstrom J, Loring RH. Determination of nicotinic receptor subtypes in chick retina using monoclonal antibodies and ³H-epibatidine. *Med Chem Res.* 1994;4:528–537.
 30. Bullock AE, Clark AL, Grady SR, et al. Neurosteroids modulate nicotinic receptor function in mouse striatal and thalamic synaptosomes. *J Neurochem.* 1997;68:2412–2423.